Proceedings of the International Conference on Oxide Materials for Electronic Engineering, May 29–June 2, 2017, Lviv

Electrical, Electromechanical and Piezoelectric Properties of $Ca_3TaGa_3Si_2O_{14}$ Resonators at Elevated Temperatures

Yu. Suhak[a,*], M. Schulz[a], A. Sotnikov[b], H. Schmidt[b] and H. Fritze[a]

[a]Institute of Energy Research and Physical Technologies, Clausthal University of Technology, Am Stollen 19B, 38640, Goslar, Germany

[b]SAWLab Saxony, Leibniz Institute for Solid State and Materials Research (IFW Dresden), Helmholtzstr. 20, 01069, Dresden, Germany

The electrical conductivity, resonance frequency and piezoelectric strain constants are determined for ordered piezoelectric $Ca_3TaGa_3Si_2O_{14}$ (CTGS) single crystals from room temperature to 900 °C. The latter result from three independent methods, namely resonant, ultrasonic pulse-echo, and laser Doppler vibrometry techniques, which allows validating the results. Further, the long-term behaviour of fundamental materials properties including electrical conductivity and resonance frequency are examined at 1000 °C for CTGS crystals, grown by different manufacturers. After an initial period of about 500 h, the conductivity is found to remain nearly constant for at least 1500 h. In a period of 2000–5000 h a decrease of conductivity by only 20% is observed. The resonance frequency is found to decrease almost linearly in a period of 500–5000 h for all investigated samples.

DOI: 10.12693/APhysPolA.133.1069

PACS/topics: 77.65.Bn, 77.84.–s, 43.58.Bh, 07.20.Ka

1. Introduction

High temperature piezoelectric sensors suited for harsh environments are currently in high demand for a wide range of industrial applications including gas sensing or mass detection in nanogram scale. Many of the intensively investigated materials have however restrictions for high-temperature application. Thus, the maximum operating temperature for most commonly used materials such as quartz (SiO_2) and non-stoichiometric lithium niobate ($LiNbO_3$) is determined by the phase transformation at 573 °C [1, 2] and decomposition at about 300 °C [3, 4] respectively.

Langasite family crystals attract significant attention for high-temperature piezoelectric sensing applications, have no phase transformation up to their melting point (1300–1500 °C) [5] and exhibit good piezoelectric properties [6–9]. Their crystal structure has four different cation sites and can be described by the general formula $A_3BC_3D_2O_{14}$. In langasite ($La_3Ga_5SiO_{14}$, LGS) Ga^{3+} ions fully occupy both B and C sites, and half of the D sites in a random way, which leads to the structural disorder and increased losses [10].

$Ca_3TaGa_3Si_2O_{14}$ (CTGS) exhibits a fully ordered structure, resulting in lower conductivity and loss, compared to those of LGS [6, 11]. However, the CTGS material properties at elevated temperatures have not been completely studied up to now. In particular, its piezoelectric constants are determined mainly at room temperature and the published values exhibit a large divergence among the publications [12–15]. Further, the stability of the fundamental properties of CTGS at elevated temperatures over long periods of time is not examined, although those investigations are crucial in respect of CTGS sensor applications.

This work focuses on the determination of piezoelectric constants of CTGS from ambient temperature to 900 °C, using the resonant method according to [16, 17] and the ultrasonic pulse-echo method. Additionally, the piezoelectric constant d_{11} is determined by the laser Doppler vibrometry (LDV) technique. The application of three independent methods to determine the same constants is used here for validating the results.

Further, the fundamental properties of CTGS resonators such as electrical conductivity and resonance frequency are examined as a function of temperature and time. Changes in properties at elevated temperatures over long time periods are of particular interest.

2. Methods

CTGS crystals belong to the symmetry class 32 and therefore have two independent piezoelectric strain constants d_{11} and d_{14} [18]. These constants are determined by the resonant method according to [16, 17] and by the pulse echo method in a temperature range from room temperature to 900 °C and to 800 °C, respectively. Additionally, the piezoelectric constant d_{11} is measured from room temperature to 900 °C by the LDV method. Further, the electrical conductivity and the resonant frequency as a function of temperature and time are analyzed by impedance measurements.

2.1. Resonant method

The resonant technique refers to the IEEE dynamic methods and is suited for the material constants determination in low loss crystals [16]. Two $(XYt)+\alpha$ rods are

*corresponding author; e-mail: yuriy.suhak@tu-clausthal.de

operated in the length-extensional mode. Their electrical impedance is acquired in the vicinity of the resonant frequency by a high speed impedance analyzer (Agilent E5100A). From these data the resonance and antiresonance frequencies are extracted. This procedure is described in more detail in [19]. The orientation notation used here follows the IEEE Standard on Piezoelectricity [16].

The piezoelectric strain constants d_{11} and d_{14} can be determined, using the following equations:

$$d_{11}(\alpha) = -d_{12}(\alpha) = \sqrt{k_{12}^2(\alpha)\,\varepsilon_{11} S_{11}}, \tag{1}$$

$$d_{12}(\alpha) = -d_{11}\cos^2\alpha + d_{14}\sin\alpha\cos\alpha, \tag{2}$$

$$\frac{k_{12}^2(\alpha) - 1}{k_{12}^2(\alpha)} = \frac{\tan\left(\frac{\pi}{2}\frac{f_A(\alpha)}{f_R(\alpha)}\right)}{\frac{\pi}{2}\frac{f_A(\alpha)}{f_R(\alpha)}}, \tag{3}$$

$$S_{11} = \frac{1}{4\rho(l f_R)^2} \quad , \tag{4}$$

where k_{12} is the electromechanical coupling coefficient, ε_{11} is the dielectric permittivity, S_{11} is the elastic compliance, f_R and f_A are the corresponding resonance and antiresonance frequencies of the rods, respectively, ρ is the CTGS density and l is the length of the $(XYt) + \alpha$ rod.

As mentioned above, the method can be applied only for low loss materials and is based on the approximation that the resonance frequency f_R and the series resonance frequency f_S as well as the antiresonance frequency f_A and the parallel resonance frequency f_P are equal, respectively [16]. Our measurements show that the relative differences $(f_S - f_R)/f_S$ and $(f_A - f_P)/f_A$ for a CTGS resonator at 900 °C are only 10 ppm and 1000 ppm, respectively, which justifies the usage of the resonant methods for determination of the piezoelectric constants.

2.2. Pulse-echo method

Measurements of the bulk acoustic wave velocities propagating along certain crystallographic directions are carried out by a RITEC Advanced Ultrasonic Measurement System RAM-5000. Using phase detectors, the system allows measurements of pulse propagation time with an accuracy of about 10^{-4}. To generate longitudinal and shear ultrasonic waves, $Y + 36°$- and X-cut $LiNbO_3$ transducers are used, which are operated far off the samples resonance frequency. Piezoelectric constants are derived using a system of relations between sound velocities measured at characteristic directions for different acoustic modes (see e.g. [20]). A more detailed description of the pulse-echo method can be found in a previous publication [21].

2.3. Laser Doppler vibrometry method

The piezoelectric strain constant d_{11} of the X-cut CTGS sample is also determined by the laser Doppler vibrometer (Polytec OFV-505), which enables to detect displacements in the sub-nanometer range at frequencies from about 1 Hz to 10 MHz. The sample is excited at a frequency of 60 Hz, which is far below its resonance frequency. The external voltage U applied to the CTGS sample is 200 V. The piezoelectric constant d_{11} is than calculated, using the following equation:

$$d_{11} = \frac{\Delta \mathrm{x}}{U}, \tag{5}$$

where Δx is the displacement of the sample surface. The measurement procedure is described in more detail in [22].

2.4. Impedance spectroscopy

The determination of the electrical conductivity is performed by ac impedance spectroscopy in the frequency range from 1 Hz to 1 MHz using an impedance/gain-phase analyzer (Solartron 1260). An electrical equivalent-circuit model consisting of a constant phase element connected in parallel with the bulk resistance R_B is fitted to the experimental data. The bulk conductivity σ is then calculated through the relation

$$\sigma = \frac{t}{A}\frac{1}{R_B}, \tag{6}$$

where t and A are the thickness of the sample and the electrode area, respectively.

The resonant properties are characterized with a high-speed network analyzer (Agilent E5100A). Thereby, the electrical impedance is examined in the vicinity of the resonance frequency and subsequently transformed into admittance $Y = Z^{-1}$. Fitting a Lorentz function to the resonant peaks of the real part of the admittance is done to extract the resonance frequency. This procedure is described in more detail in [19].

3. Samples and experimental details

The high-temperature measurements are carried out in air at atmospheric pressure. The samples are heated at a rate of 1 K/min starting at room temperature. The maximum temperature is defined individually for each type of sample and experiment. The long-term measurements are performed at 1000 °C. The mass density ρ of CTGS used here is determined by the Archimedes method and equals 4620 kg/m^3 [13].

The measurements according to the resonant method are performed on two rods with the orientation of $(XYt) + 0°$ and $(XYt) - 47°$ and dimensions of $2 \times 0.5 \times 10$ mm^3. The samples are prepared from the Czochralski-grown CTGS crystal, provided by the Institute for Crystal Growth (IKZ), Berlin, Germany. The orientation accuracy is within 0.5°. The samples are coated with about 300 nm thick platinum electrodes by pulsed laser deposition (PLD).

The LDV measurements are carried out on an X-cut sample with the dimensions of $10 \times 10 \times 0.5$ mm^3, manufactured from the same crystal. The platinum electrodes are prepared by the PLD technique, too. The sample is

then mounted in an alumina sample holder and placed in a tube furnace which allows heating up to 1400 °C. The LDV is placed in front of a tube furnace. The minimum achieved resolution of the displacement is at least 100 pm. The position of the laser spot on the sample surface is controlled by a specially equipped camera.

The pulse-echo measurements are performed on the Czochralski grown crystals, provided by Fomos-Materials, Moscow, Russia. For this purpose crystal cubes of $7 \times 7 \times 7$ mm^3 are prepared in two different orientations: (i) with the edges parallel to the main crystallographic axes X, Y, Z, and (ii) rotated by $\pm 45°$ around the X axis. Orientation accuracy is within 0.1°.

For the impedance spectroscopy Y-cut plates with 10 mm diameter and 0.3 mm thickness are manufactured from the Czochralski-grown CTGS crystals, provided by IKZ, FOMOS-Materials and SICCAS, Shanghai, China. For these samples, about 3 µm thick keyhole-shaped platinum electrodes are deposited by screen printing (print ink: Ferro Corporation, No. 6412 0410). The resonators are preannealed at 1000 °C for about 30 min.

4. Results and discussion

4.1. Piezoelectric constants

The temperature-dependent piezoelectric strain constants of CTGS single crystals, determined by the methods, described in Sects. 2.1–2.3, are shown in Fig. 1. As it can be seen from Fig. 1, the temperature dependence of the constant d_{11} is similar within the entire temperature range of investigation, except for some decrease observed at 400 °C for the LDV measurements. The latter value, however, lies within the uncertainty of the measurement of this method, which is 10% according to our calculations. The absolute values of d_{11}, determined by the resonant and the pulse-echo methods are also showing slight differences, which are smaller than 5%. These results are in a good agreement with the calculated uncertainty for d_{11}, which is below 6% for the resonant method.

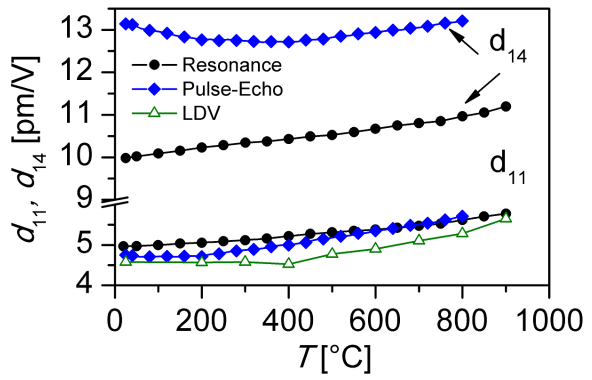

Fig. 1. Piezoelectric strain constants d_{11} and d_{14} as a function of temperature.

The temperature dependence of the piezoelectric strain constant d_{14}, which is also presented in Fig. 1, shows a divergence of approximately 18%. However, it should be noted that the values of d_{14} (or of corresponding piezoelectric stress constant e_{14}) reported by other authors [12–15] exhibit a divergence of more than 50% at room temperature, respectively. The uncertainty for the constant d_{14} is below 8% in case of the resonant measurements.

4.2. Temperature-dependent conductivity and resonant properties

The temperature-dependent electrical conductivities of the CTGS samples from different manufacturers are shown as the Arrhenius plot in Fig. 2. As it can be seen from the figure, they exhibit different values in the measured temperature range. Thus, the electrical conductivity of the sample, manufactured from IKZ crystal is lower by one order of magnitude as compared to SICCAS sample. Therefore the conduction-related loss is expected to be significantly lower in IKZ resonators.

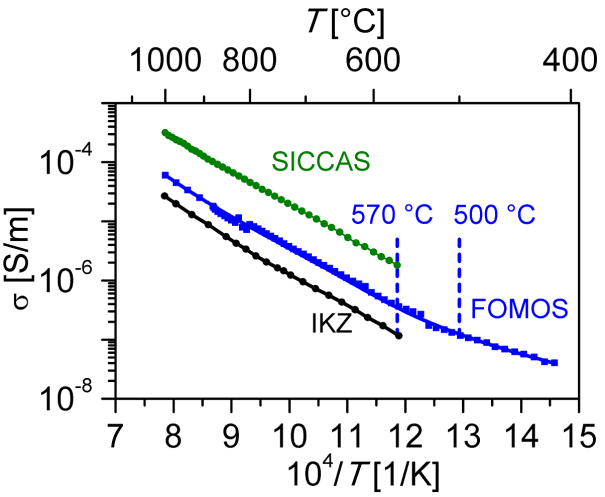

Fig. 2. Temperature dependent electrical conductivity of different CTGS samples.

The data for the FOMOS sample are linear in this presentation below 500 °C. After a transition temperature range of 500–570 °C, observed conductivity increase is linear again, however the slope changes (see mark in Fig. 2). It means that the conductivity is governed by a different process, than that at lower temperatures. It should be noted that a similar behaviour was observed previously for LGS crystals [23, 24]. It is shown in [23], that at temperatures below 700 °C electronic conduction governs the conductivity in LGS, while at higher temperatures ionic conduction dominates. The data for the IKZ and SICCAS samples are linear in the Arrhenius presentation within all the measured temperature range.

The obtained results enable the determination of the activation energy E_A, using the relation

$$\sigma = \sigma_0 \exp\left(\frac{-E_A}{k_B T}\right), \tag{7}$$

where σ_0, k_B, and T are a pre-exponential coefficient, the Boltzmann constant and the temperature, respectively.

Activation energies obtained by fitting the data to (7) and the temperature ranges for fitting are summarized in Table I.

TABLE I

Activation energies and pre-exponential coefficients for conductivity at different temperatures.

	T [°C]	E_A [eV]	σ_0 [S/m]
FOMOS	420–500	0.75±0.03	$(1.2\pm0.05)\times10^{-2}$
FOMOS	570–1000	1.16±0.05	1.97±0.08
IKZ	570 - 1000	1.15±0.05	1.1±0.05
SICCAS	570–1000	1.12±0.05	6.9±0.2

Figure 3 presents the temperature dependent resonance frequency of the fundamental mode of Y-cut CTGS resonators relative to that at 150 °C. Resonant peaks are observed even at 1270 °C for the FOMOS sample, which is already close to the CTGS melting temperature (1350 °C). The frequency shifts of the IKZ and SICCAS resonators are measured up to 1000 °C only, however it is most likely that the resonant peaks could be observed with further increase of the temperature, too. As follows from Fig. 3 the resonance frequency of all samples decreases approximately linearly with temperature over the entire measured range, which is of practical importance for e.g. sensing applications.

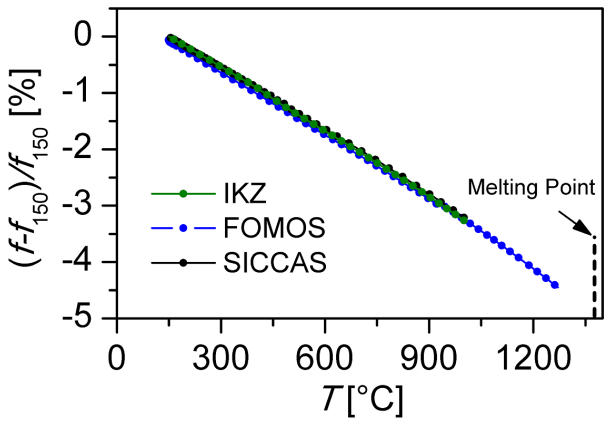

Fig. 3. Temperature-dependent relative change of the resonance frequency of different CTGS samples.

4.3. Time-dependent conductivity and resonant properties

In order to determine the stability of the CTGS resonators, their electrical conductivity and resonance frequency are examined at 1000 °C in air during 5000 h. The time dependent electrical conductivities of different CTGS specimens are shown in Fig. 4. The initial conductivities are 2.6×10^{-5} S/m, 5.1×10^{-5} S/m, and 3.1×10^{-4} S/m for IKZ, FOMOS, and SICCAS samples, respectively. Those values are in a good agreement with the short-term temperature dependent measurements (see Fig. 2). However, within approximately 500 h of thermal treatment, the electrical conductivity of IKZ and FOMOS samples increases and reaches the values of 1.65×10^{-4} S/m and 1.75×10^{-4} S/m, respectively. SICCAS sample also shows the conductivity increase, however the changes are slower, reaching the value of 5.3×10^{-4} S/m after 1000 h of thermal treatment. The origin of this conductivity increase of the CTGS samples at the initial stage is a subject for further investigations.

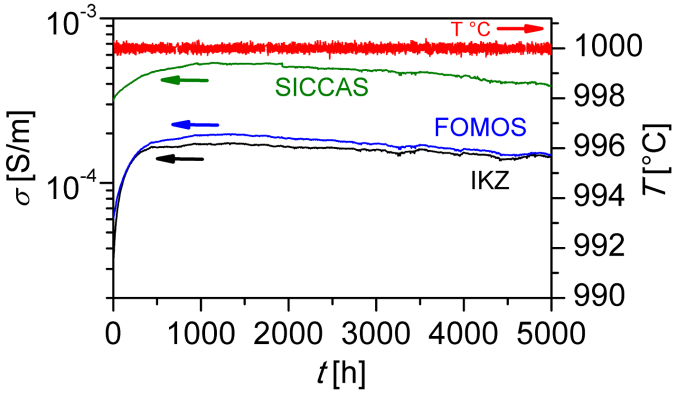

Fig. 4. Time dependent electrical conductivity of different CTGS samples.

After this first period of time the conductivity of all specimens remains nearly constant within the next 1500 h of thermal treatment. In the period of 2000–5000 h, the measured electrical conductivity of the samples decreases by about 20%. This decrease is potentially caused by electrode degradation. However, this hypothesis also requires further investigation. It should be noted that the similar conductivity decrease for about 15% was observed previously for LGS sample after 5000 h of thermal treatment under the same conditions [11].

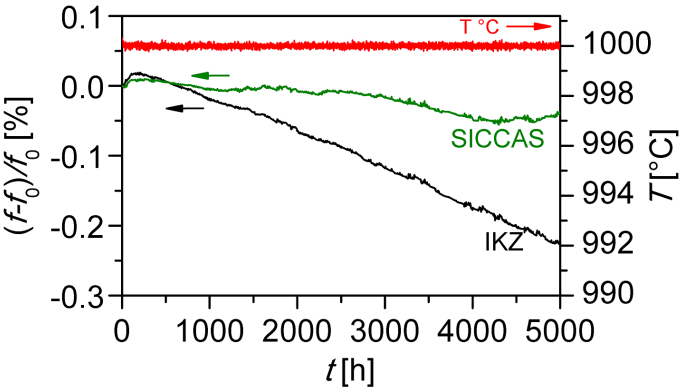

Fig. 5. Time-dependent relative change of the resonance frequency of different CTGS samples.

Figure 5 shows the change of the fundamental resonance frequency of Y-cut resonators prepared from IKZ and SICCAS crystals as a function of time during annealing at 1000 °C, relative to that at the initial point of measurements at 1000 °C (f_0). As can be seen from Fig. 5, a frequency shift is observed for the IKZ resonator during the first 500 h of investigation. The shift occurs

in the same time span as the time-dependent conductivity changes (see Fig. 4). Here, a correlation must be investigated in concert with the explanation of the conductivity change. After this period of time the resonance frequency steadily decreases, reaching a relative shift of 0.2% at 5000 h, comparing to that of f_0. The behaviour of SICCAS resonator is similar, however its resonance frequency changes in the ppm range, reaching the value of only 0.05% at 5000 h, in comparison to f_0.

5. Conclusions

The piezoelectric constants are determined for CTGS single crystals in a temperature range from room temperature to 900 °C. Further, the fundamental properties of CTGS resonators such as electrical conductivity and resonance frequency are examined as a function of temperature and time. It is shown that the piezoelectric strain constant d_{11} exhibits the same temperature dependence for resonant, pulse-echo, and LDV measurements, the absolute values of the constant however somewhat differ. Observed divergences lie within the measurement error.

Measurements of the temperature dependent electrical conductivity show that values for IKZ CTGS samples are almost one order of magnitude smaller than those of SICCAS. The long-term behaviour of CTGS shows that its conductivity exhibits essential drift during the initial stage of the experiment. After this period of time these properties remain nearly stable for next 1500 h; some conductivity decrease is observed in the period of 2000–5000 h.

The fundamental resonance frequency decreases almost linearly with the temperature for all investigated samples. It was found that the resonance frequency of SICCAS resonator is changed by about 500 ppm during 5000 h of thermal treatment at 1000 °C.

Acknowledgments

Research grant from the German Research Foundation (DFG: FR 1301/21-1 and SO 1085/2-1) made this work possible. Authors from Clausthal University of Technology acknowledge the support from the Energie-Forschungszentrum Niedersachsen.

References

[1] J. Haines, O. Cambon, D. Keen, M. Tucker, M. Dove, *Appl. Phys. Lett.* **81**, 2968 (2002).

[2] R.W. Cernosek, J.R. Bigbie, M.T. Anderson, J.H. Small, P.S. Sawyer, *Solid-State Sensor and Actuator Workshop*, Hilton, Head Island (SC) 1998

[3] D.P. Birnie III, *J. Mater. Sci.* **28**, 302 (1993).

[4] D. Damjanovic, *Curr. Opin. Solid State Mater. Sci.* **3**, 469 (1998).

[5] K. Shimamura, H. Takeda, T. Kohno, T. Fukuda, *J. Cryst. Growth* **163**, 388 (1996).

[6] S. Zhang, Y. Zheng, H. Kong, J. Xin, E. Frantz, T.R. Shrout, *J. Appl. Phys.* **105**, 114107 (2009) .

[7] F. Yu, Sh. Zhang, X. Zhao, D. Yuan, L. Qin, Q.-M. Wang, T.R. Shrout, *J. Appl. Phys.* **109**, 114103 (2011).

[8] H. Fritze, H.L. Tuller, G. Borchardt, T. Fukuda, *MRS Proc.* **604**, 65 (1999).

[9] H.L. Tuller, H. Fritze, US Patent 6370955, 2002.

[10] H. Ohsato, T. Iwataki, H. Morikoshi, *Trans. Electr. Electron. Mater.* **13**, 171 (2012).

[11] Yu. Suhak, M. Schulz, H. Wulfmeier, W.L. Johnson, A. Sotnikov, H. Schmidt, S. Ganschow, D. Klimm, H. Fritze, *MRS Adv.* **1**, 1513 (2016).

[12] X. Shi, D. Yuan, X. Yin, A. Wei, Sh. Guo, F. Yu, *Solid State Commun.* **142**, 173 (2007).

[13] A. Sotnikov, H. Schmidt, M. Weihnacht, O. Buzanov, S. Sakharov, *Proc. IEEE Int. Ultrason. Symp.*, 1688 (2013).

[14] Yu.V. Pisarevsky, B.V. Mill, N.A. Moiseeva, A.V. Yakimov, in: *Proc. 18th European Frequency and Time Forum* Guildford (UK) 2004, p. 216.

[15] S. Biryukov, H. Schmidt, A. Sotnikov, M. Weihnacht, S. Sakharov, O. Buzanov, *Proc. IEEE Int. Ultrason. Symp.*, 882 (2014).

[16] IEEE Standard on Piezoelectricity, *ANSI/IEEE Standards* **176**, 1 (1987).

[17] M. Schulz, H. Fritze, *Renew. Energy* **33**, 336 (2008).

[18] T. Ikeda, *Fundamentals of piezoelectricity*, Oxford University Press, Oxford 1990.

[19] T. Schneider, D. Richter, S. Doerner, H. Fritze, P. Hauptmann, *Sens. Actuat. B* **111**, 187 (2005).

[20] J.A. Kosinski, R.A. Pastore, E. Bigler, M. Pereira da Cunha, D.C. Malocha, J. Detaint, *Proc. IEEE Int. Freq. Contr. Symp.*, 278 (2001).

[21] Yu. Suhak, M. Schulz, A. Sotnikov, H. Schmidt, S. Ganschow, S. Sakharov, H. Fritze, *Integr. Ferroelectr.*, in press.

[22] S. Schmidtchen, D. Richter, H. Fritze, *Sens. Actuators B* **187**, 247 (2013).

[23] H. Fritze, *J. Electroceram.* **17**, 625 (2006).

[24] W.L. Johnson, M. Schulz, H. Fritze, *IEEE Trans. Ultrason. Ferroelect. Freq. Control* **61**, 1433 (2014).